CANCER

TOPK inhibitor induces complete tumor regression in xenograft models of human cancer through inhibition of cytokinesis

Yo Matsuo,[1]* Jae-Hyun Park,[2]* Takashi Miyamoto,[1] Shinji Yamamoto,[1] Shoji Hisada,[1] Houda Alachkar,[2] Yusuke Nakamura[2†]

TOPK (T–lymphokine-activated killer cell–originated protein kinase) is highly and frequently transactivated in various cancer tissues, including lung and triple-negative breast cancers, and plays an indispensable role in the mitosis of cancer cells. We report the development of a potent TOPK inhibitor, OTS964 {(*R*)-9-(4-(1-(dimethylamino)propan-2-yl)phenyl)-8-hydroxy-6-methylthieno[2,3-*c*]quinolin-4(5*H*)-one}, which inhibits TOPK kinase activity with high affinity and selectivity. Similar to the knockdown effect of TOPK small interfering RNAs (siRNAs), this inhibitor causes a cytokinesis defect and the subsequent apoptosis of cancer cells in vitro as well as in xenograft models of human lung cancer. Although administration of the free compound induced hematopoietic adverse reactions (leukocytopenia associated with thrombocytosis), the drug delivered in a liposomal formulation effectively caused complete regression of transplanted tumors without showing any adverse reactions in mice. Our results suggest that the inhibition of TOPK activity may be a viable therapeutic option for the treatment of various human cancers.

INTRODUCTION

Cancer is a major public health problem in the developed countries and will become the most serious life-threatening disease worldwide in the near future. In particular, lung cancer is the leading cause of cancer-related death and the second most common cancer in the United States (*1*). Breast cancer is the most common cancer in females, and it is estimated that one in eight women in the United States will develop breast cancer in her lifetime (*2*). Advances in cancer treatment by molecular-targeted therapies such as imatinib, gefitinib, and trastuzumab were expected to improve cancer cure rates and also to reduce severe adverse reactions because of the high specificity of the targeted molecules, which are expressed and have critical roles in cancer cells but not in normal cells. However, in most of these cases, the clinical effect was found to be limited and did not last for a long time period because of the acquired resistance of tumor cells. Furthermore, these molecules often cause on-target and/or off-target severe toxicity (*3*). Therefore, development of more target-specific therapy with minimum toxicity is warranted to extend disease-free survival and improve the quality of life of cancer patients.

For the treatment of breast cancer, drugs targeting two molecules, estrogen receptor (ER) and human epidermal growth factor receptor 2 (HER2), are well established and are considered to be the gold standard therapeutics for treating ER- and HER2-positive breast cancers, respectively (*4*). However, there are very limited treatment options available to patients who become resistant to the above treatments and for those with cancers that do not express the appropriate receptors, such as triple-negative breast cancers (TNBCs).

TOPK (T–lymphokine-activated killer cell–originated protein kinase, also known as PBK or PDZ-binding kinase) is a Ser/Thr protein kinase that is highly expressed in many types of human cancer, including breast and lung cancers (*5*–*7*). We previously suggested that TOPK might be a promising molecular target for drug development because TOPK is not expressed in vital organs and plays an important role in breast cancer cell mitosis (*8*). A recent study of genome-wide expression profiling determined that TOPK is very highly up-regulated in most TNBCs (*9*). Moreover, TOPK was included in the "consensus stemness ranking signature" gene list that is up-regulated in cancer stem cell–enriched tumors and is associated with poor prognosis in multiple types of cancer (*10*). These findings further support the concept that TOPK is an attractive molecular target for treatment of a wide range of human cancers.

Our previous drug development efforts, including high-throughput compound library screening and extensive structure-activity relationship (SAR) studies, discovered that some thieno[2,3-*c*]quinolone compounds can inhibit the activity of TOPK kinase (*11*). Among them, compound OTS514 {(*R*)-9-(4-(1-aminopropan-2-yl)phenyl)-8-hydroxy-6-methylthieno[2,3-*c*]quinolin-4(5*H*)-one)}was identified as an extremely potent TOPK inhibitor. In vitro cell-based assays revealed that OTS514 strongly suppressed the growth of TOPK-positive cancer cells. Mouse xenograft studies with human lung cancer cells demonstrated the in vivo efficacy of OTS514 but found that the compound also caused severe hematopoietic toxicity [reduction of red blood cells (RBCs) and white blood cells (WBCs) associated with marked increase in platelets]. Hence, we considered liposomal formulations of the compound and its derivatives for clinical application.

The liposomal drug delivery system has been widely applied in the clinic and provides an opportunity to increase drug solubility and stability in circulation, as well as to reduce the side effects of anticancer agents in nontarget tissues. In addition, the liposomal formulation can increase drug concentrations in tumors by the "enhanced permeability and retention (EPR)" effect that enhances preferential extravasation of drugs from tumor vessels and accumulation in the tumor area (*12*). For example, the liposome-coated doxorubicin Doxil was the first liposomal pharmaceutical product approved for the treatment of cancer patients, including those with

[1]OncoTherapy Science Inc., Kawasaki, Kanagawa 213-0012, Japan. [2]Department of Medicine, The University of Chicago, Chicago, IL 60637, USA.
*These authors contributed equally to this work.
†Corresponding author. E-mail: ynakamura@bsd.uchicago.edu

ovarian cancer and Kaposi sarcoma. Because of the improvement of anticancer efficacy and the reduction of toxicity, numerous liposome-coated drugs are under development for cancer treatment (*13*).

In the present study, we report that the liposomal formulation enhanced the antitumor effect with substantial reduction of the hematopoietic toxicity. Exploration of OTS514-analog compounds revealed that OTS964 {(*R*)-9-(4-(1-(dimethylamino)propan-2-yl)phenyl)-8-hydroxy-6-methylthieno[2,3-*c*]quinolin-4(5*H*)-one}, a dimethylated derivative of OTS514, exhibited excellent in vivo efficacy with liposomal formulation. The liposomal OTS964 caused complete regression of tumors without any detectable toxicity in the xenograft models. Biological analyses of the tumors revealed that treatment with the liposomal formulation of OTS964 effectively induced apoptosis in cancer cells. These results suggest that the liposomal TOPK inhibitor may be a promising molecular-targeted therapy, which could be applied to treat cancer patients whose tumors express high amounts of TOPK.

RESULTS

Correlation of *TOPK* overexpression with poor prognosis of cancer patients

Accumulating reports have suggested oncogenic roles of TOPK in a wide range of human cancers. To validate the clinical role of TOPK expression in human malignancies, we correlated the expression of *TOPK* with overall survival of cancer patients in a published microarray database (*14*, *15*). In the Kaplan-Meier survival analyses of this data set, which included more than 1000 cancer patients, we found that higher *TOPK* expression was significantly correlated with poor prognosis in breast and lung cancer patients ($P = 6.9 \times 10^{-9}$ and $P = 2.1 \times 10^{-15}$, respectively; fig. S1). This finding suggests that TOPK inhibitors may be able to improve clinical outcome of breast and lung cancer patients who have tumors with high *TOPK* expression.

Development of TOPK inhibitor OTS514

We had previously identified a thieno[2,3-*c*]quinolone compound, OTS514, as a highly potent TOPK inhibitor (Fig. 1A). The compound inhibited TOPK kinase activity with a median inhibitory concentration (IC_{50}) value of 2.6 nM (*11*). To confirm the specificity of OTS514 compound against TOPK, we used a panel of 60 diverse human protein kinases (table S1). The activity of each kinase was measured after a 2-hour incubation with 0.2 μM OTS514. The highest inhibition was observed for TOPK (83.5% inhibition), whereas the mean and the SD of the inhibitory effects against other kinases were 11.5 and 18.5%, respectively, indicating the specificity of the TOPK inhibitory effect of this compound.

We examined TOPK expression in cancer cell lines derived from various cancer types, such as lung cancer (A549, LU-99), breast cancer (DU4475, MDA-MB-231, and T47D), Burkitt lymphoma (Daudi), bladder cancer (UM-UC-3), colon cancer (HCT-116 and HT29), gastric cancer (MKN1 and MKN45), liver cancer (HepG2), pancreatic cancer (MIAPaca-2), and prostate cancer (22Rv1). High expression of TOPK was observed in all of these cell lines except HT29 (Fig. 1B). We then examined the growth inhibitory effects of the compound on each cell line (fig. S2) and found strong growth inhibitory effects with low IC_{50} values ranging from 1.5 to 14 nM for the TOPK-positive cancer cell lines. On the other hand, the IC_{50} value for HT29 cells, in which TOPK expression was hardly detectable, was significantly higher at 170 nM ($P = 5.92 \times 10^{-11}$; Fig. 1C).

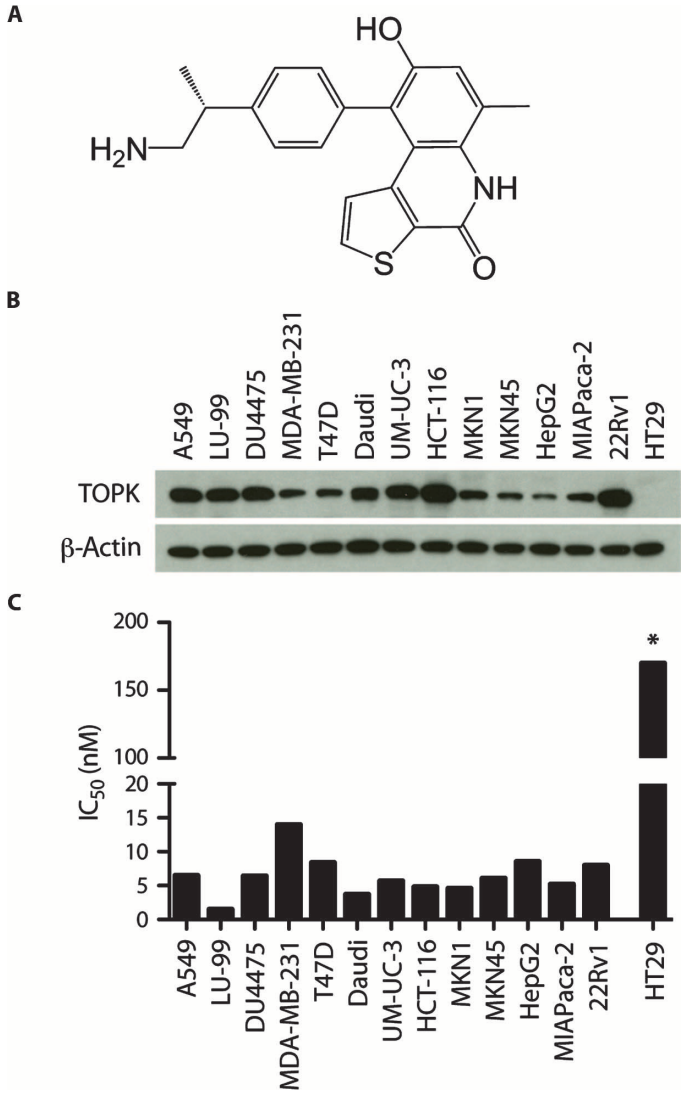

Fig. 1. In vitro antiproliferative activity of OTS514. (**A**) Chemical structure of OTS514. (**B**) Western blot shows expression of TOPK in cancer cell lines. (**C**) Graph indicates IC_{50} values of OTS514 in 13 TOPK-positive cancer cell lines and a TOPK-negative cancer cell line, HT29. $^*P = 5.92 \times 10^{-11}$.

In vivo efficacy of OTS514

Because TOPK is commonly expressed in lung cancers (*6*) and its high expression is associated with poor prognosis for lung cancer patients (fig. S1), we first investigated the in vivo antitumor effect of OTS514 in a xenograft model of A549 cells (TOPK-positive lung cancer cells). OTS514 was administered to mice bearing A549 cells after the tumor size reached about 200 mm^3. The tumor size was measured as a surrogate marker of drug response, and the percentage of tumor growth inhibition (TGI) was calculated according to the formula $[1 - (T - T_0)/(C - C_0)] \times 100$, where T and T_0 are the mean tumor volumes at day 15 and day 1, respectively, for the experimental group, and C and C_0 are those for the vehicle control group. Intravenous administration of free OTS514 at 1, 2.5, and 5 mg/kg once a day for 2 weeks resulted in TGI of 5.7, 43.3, and 65.3% on day 15, respectively (Fig. 2A), without any body weight loss (Fig. 2B). However, we observed some hematopoietic

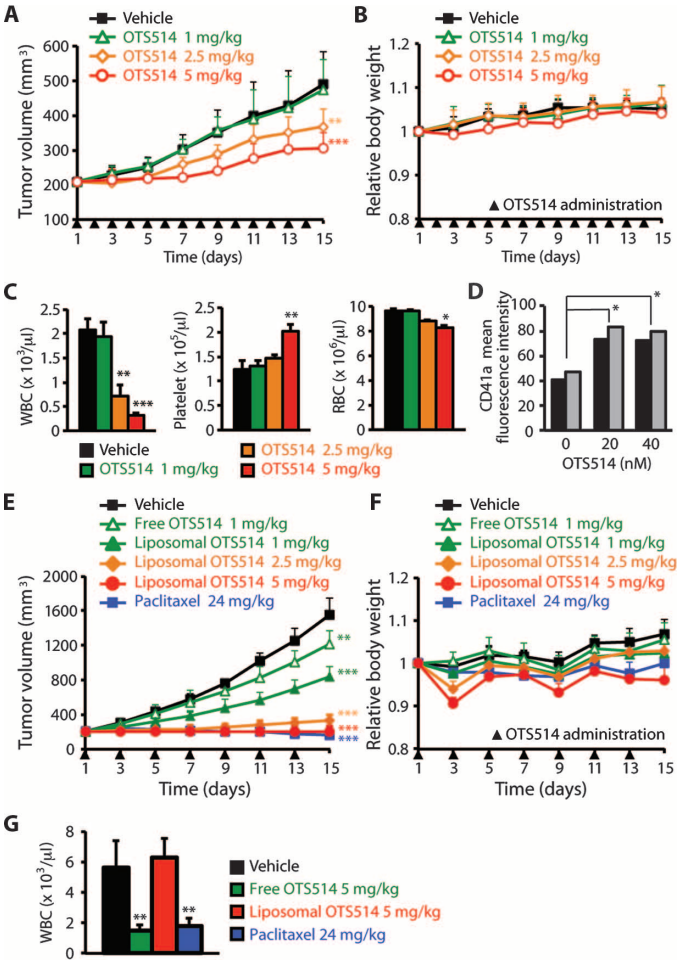

Fig. 2. In vivo efficacy of OTS514 in lung cancer xenograft models. (**A** to **C**) Nude mice bearing A549 ($n = 8$) were intravenously treated with vehicle control or free OTS514 once every day for 2 weeks. Mean tumor volumes ± SD (A) and mean relative body weights ± SD (B) in comparison with the mean body weight just before the administration (day 1) are shown. Counting of WBCs, platelets, and RBCs was performed with Sysmex XT-1800iV Analyzer (C). (**D**) After treatment with OTS514, differentiation of HSCs to megakaryocytes was assessed by staining with CD41a. (**E** to **G**) Nude mice bearing LU-99 ($n = 6$) were intravenously treated with vehicle control, free OTS514, or liposomal OTS514 every 2 days for 2 weeks or paclitaxel at days 1, 4, 8, and 11. Mean tumor volumes ± SD (E) and mean relative body weights ± SD (F) in comparison with the mean body weight just before the administration (day 1) are shown. WBCs were counted with a cell counting chamber after administration of vehicle control, free OTS514 (5 mg/kg), or liposomal OTS514 (5 mg/kg) every 2 days for 2 weeks, or paclitaxel (24 mg/kg) at days 1, 4, 8, and 11 (G). *$P < 0.05$, **$P < 0.01$, or ***$P < 0.001$ by t test. Original data and exact P values are provided in table S2.

toxicity, with mild anemia and relatively severe leukocytopenia, whereas the number of peripheral platelets was increased in a dose-dependent manner (Fig. 2C). The results suggested that the inhibitor causes dysfunction in the differentiation process of hematopoietic stem cells (HSCs) to WBCs and RBCs but may enhance the differentiation of HSCs to megakaryocytes and platelets. To address this question, we examined the effect of OTS514 on differentiation of human HSCs by measuring the number of megakaryocytes using CD41a expression as a marker. As expected, we observed a significant increase in the megakaryocyte population after treatment with 20 or 40 nM OTS514 ($P = 0.04$ and $P = 0.02$, respectively; Fig. 2D). These results suggest that TOPK may play a critical role in the differentiation of hematopoietic stem/progenitor cells and that its inhibition might enhance differentiation to platelet lineage (megakaryocytopoiesis).

We further investigated the antitumor effect of OTS514 in another lung cancer xenograft model of LU-99 cells. Although LU-99 cells are known to grow very rapidly and are considered to be more aggressive, our in vitro data indicated that this cell line was more sensitive to OTS514 than A549 cells (Fig. 1C). OTS514 was administered to mice bearing LU-99 cancer cells after the tumor size reached about 200 mm^3. Intravenous administration of OTS514 (5 mg/kg) once a day for 2 weeks achieved good growth-suppressive effect with TGI of 104% (fig. S3A) without any body weight loss (fig. S3B). However, although the antitumor effect against LU-99 xenograft was stronger than that against A549 xenograft (Fig. 2A), the treatment still caused a significant reduction of WBCs ($P < 0.01$; fig. S3C). These results indicated that hematopoietic toxicity would be a major challenge to overcome for potent TOPK inhibitors.

In vivo application of liposomal formulation of OTS514

To enhance the antitumor effect and to reduce the hematopoietic toxicity, we generated a liposomal formulation of OTS514. The in vivo efficacy was examined by administering free and liposomal OTS514 (1 mg/kg) intravenously every 2 days for 2 weeks to mice bearing LU-99 lung cancer cells. The administration schedule was reduced to every 2 days, because prolonged circulation of the drug was expected with the liposomal formulation. In comparison with a TGI of 25.0% observed for the free OTS514 treatment, the liposomal formulation of OTS514 improved TGI to 53.0% on day 15 (Fig. 2E). Higher doses (2.5 and 5 mg/kg) of the liposomal formulation of OTS514 resulted in TGIs of 90.3 and 99.8% on day 15, respectively (Fig. 2E). This formulation caused slight reduction of body weight (Fig. 2F) but completely eliminated the hematopoietic toxicity of OTS514 (Fig. 2G).

Growth suppression of LU-99 lung cancer by liposomal OTS964

Through extensive SAR studies (*11*), we developed an OTS514-analog compound, OTS964 (Fig. 3A), which was expected to have relatively high bioavailability, although the inhibition of TOPK enzymatic activity was less effective than with OTS514. This dimethylated derivative inhibited the TOPK kinase activity with an IC_{50} value of 28 nM and maintained its specificity against TOPK, as shown by the assessment in the same set of 60 human protein kinases (table S1). OTS964 (2 μM) could inhibit 79.7% of TOPK activity, whereas the mean and the SD of the inhibitory effects against other kinases were 18.5 and 24.6%, respectively. OTS964 inhibited the growth of TOPK-positive cells with low IC_{50} values [A549 (31 nM), LU-99 (7.6 nM), DU4475 (53 nM), MDA-MB-231 (73 nM), T47D (72 nM), Daudi (25 nM), UM-UC-3 (32 nM), HCT-116 (33 nM), MKN1 (38 nM), MKN45 (39 nM), HepG2 (19 nM), MIAPaca-2 (30 nM), and 22Rv1 (50 nM)], whereas its growth inhibitory effect against TOPK-negative HT29 cancer cells was significantly ($P = 1.45 \times 10^{-4}$) weaker, with IC_{50} of 290 nM (Fig. 3B and fig. S4). Although OTS964 revealed some suppressive effect on Src family kinases, the response to OTS964 in these cancer cells was not correlated with the expression of Src family kinases c-Src, Fyn, and Lyn (fig. S5), supporting the TOPK-dependent growth inhibitory effects of OTS964. Treatment

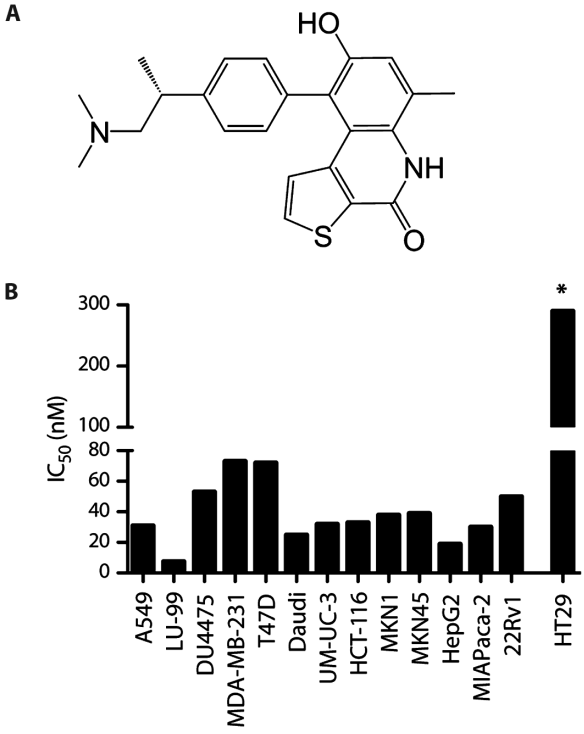

Fig. 3. In vitro antiproliferative activity of OTS964. (**A**) Chemical structure of OTS964. (**B**) Graph indicates IC_{50} values of OTS964 in 13 TOPK-positive cancer cell lines and a TOPK-negative cancer cell line, HT29. $*P = 1.45 \times 10^{-4}$.

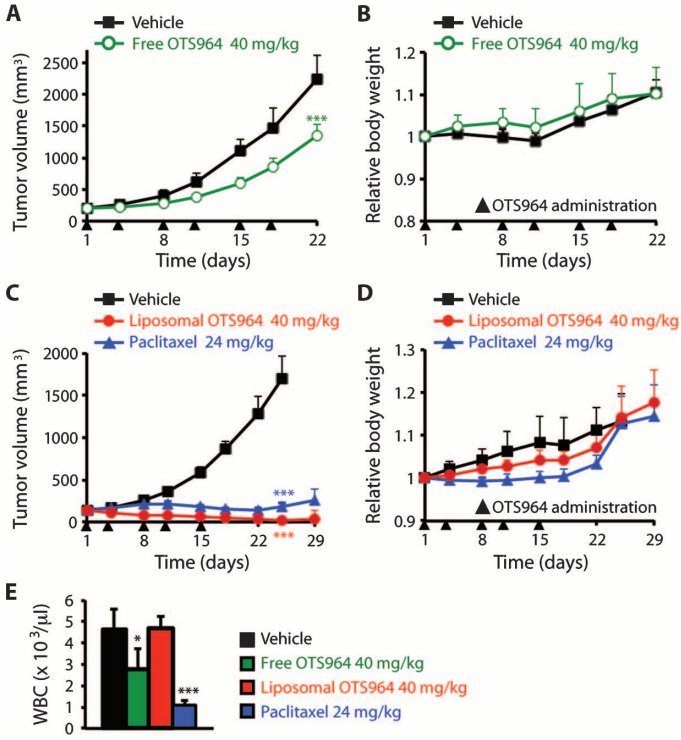

Fig. 4. In vivo efficacy of OTS964 in lung cancer xenograft models. (**A** to **D**) Nude mice bearing LU-99 were intravenously treated with vehicle control, free OTS964, liposomal OTS964, or paclitaxel. The administration doses were 40 mg/kg for free OTS964 at days 1, 4, 8, 11, 15, and 18 (A and B), 40 mg/kg for liposomal OTS964 at days 1, 4, 8, 11, and 15 (C and D), and 24 mg/kg for paclitaxel at days 1, 4, 8, 11, 15, 18, and 22 (C and D). (A and C) Mean tumor volumes ± SD ($n = 6$ per treatment group) are shown. (B and D) Mean relative body weights ± SD ($n = 6$ per treatment group) in comparison with the mean body weight just before the administration (day 1) are shown. (**E**) Counting of WBCs was performed with a cell counting chamber after final administration of free OTS964 (40 mg/kg), liposomal OTS964 (40 mg/kg), or paclitaxel (24 mg/kg). $*P < 0.05$ or $***P < 0.001$ by *t* test. Original data and exact *P* values are provided in table S2.

with OTS964 decreased autophosphorylation of TOPK (Thr^9), as well as phosphorylation of histone H3 (Ser^{10}), in both T47D and LU-99 cells (fig. S6) in concordance with our previous Western blot results after knockdown of TOPK (*5*, *8*). Moreover, time lapse imaging in T47D cells showed that treatment with OTS964 induced cytokinesis defects followed by apoptosis (video S1), which was not observed in control DMSO-treated T47D cells (video S2).

We then evaluated the in vivo efficacy of OTS964 alone or in liposomal formulation. When we administered free OTS964 intravenously at 40 mg/kg on days 1, 4, 8, 11, 15, and 18 to mice bearing LU-99 lung cancer cells, we observed a TGI of 44% on day 22 (Fig. 4A) without any body weight loss (Fig. 4B). Similar to our observation with OTS514, OTS964 treatment also enhanced the differentiation of HSCs to a megakaryocyte population (fig. S7A). Furthermore, both compounds resulted in a reduction of STAT5 (signal transducer and activator of transcription 5) protein (fig. S7B). When we administered liposomal OTS964 at 40 mg/kg on days 1, 4, 8, 11, and 15 to mice bearing LU-99 lung cancer cells after the tumor size reached about 150 mm^3 (instead of 200 mm^3 as in Fig. 4A, to allow longer monitoring of the rapidly growing LU-99 tumors; see Materials and Methods for details), we observed a TGI of 110% on day 22. The tumors continued shrinking even after the treatment and finally revealed complete regression in five of six mice examined (three mice on day 25 and two mice on day 29) (Fig. 4C) without any body weight loss (Fig. 4D). Most strikingly, this liposomal formulation did not cause any hematopoietic toxicity (Fig. 4E). Further preclinical toxicity studies in rats did not show any histopathological changes in the liver after treatment with liposomal OTS964 (fig. S8).

Antitumor effects of liposomal OTS964

To further confirm in vivo efficacy, we examined early molecular events in xenograft tumors during treatment with the liposomal formulation of OTS964. Three LU-99 xenograft mice were intravenously treated with liposomal OTS964 (40 mg/kg) or vehicle at days 1, 4, 8, and 11, and tumors were collected on day 12. We examined the cellular morphological changes and apoptosis in the LU-99 cells. Similar to the previously reported morphological changes induced by TOPK knockdown with small interfering RNA (*5*), treatment with the TOPK inhibitor induced irregular cell morphology with cytokinesis defects (Fig. 5, A and B). Treatment with the TOPK inhibitor significantly increased the number of LU-99 cells with the "intercellular bridge" ($P < 0.0001$; fig. S9), which is one of the markers indicating impaired cell division (*16*). To investigate the mode of action of OTS964, we further examined the kinase activity of TOPK, cancer cell proliferation, and apoptosis in the collected tumors on day 12. We first investigated whether administration of liposomal OTS964 effectively suppressed endogenous TOPK activity in the tumors by examining TOPK autophosphorylation and phosphorylation of histone H3, which is one of TOPK's substrates and is known

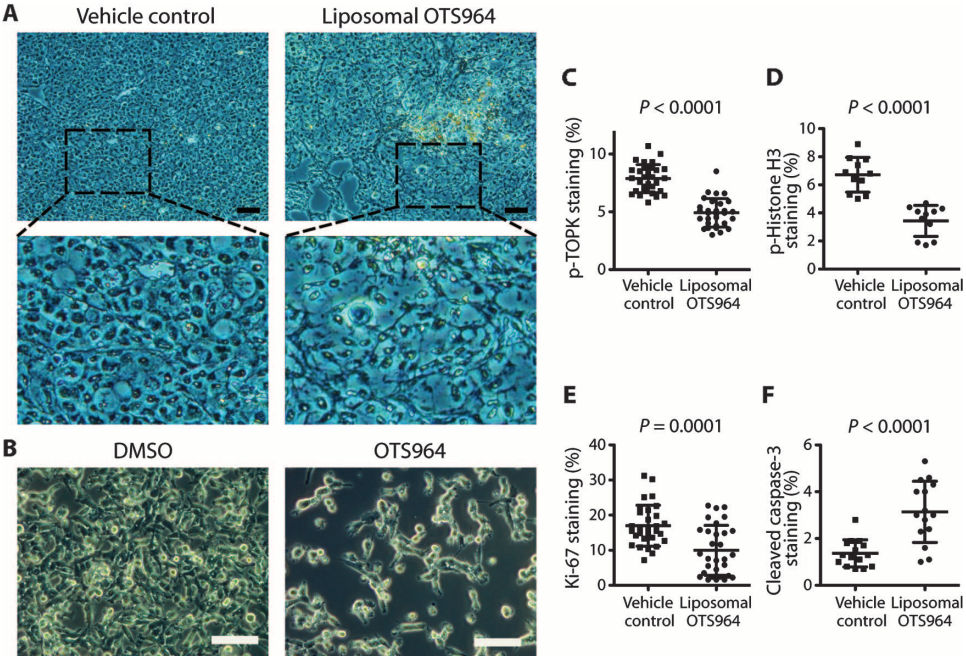

Fig. 5. Suppression of cancer cell proliferation and increase in cancer cell death after treatment with liposomal OTS964. Immunohistochemical staining and quantification of cancer cells were performed on tumor sections from LU-99 xenografts (n = 3 per group) intravenously treated with liposomal OTS964 or vehicle control. (**A**) Tumor sections were stained with methyl green to clarify cell morphology. Scale bar, 100 μm. (**B**) LU-99 cells were photographed 48 hours after treatment with 10 nM OTS964 or dimethyl sulfoxide (DMSO). Scale bar, 100 μm. (**C** to **F**) Each dot indicates the percentage of 3,3′-diaminobenzidine (DAB)–positive cells per field of interest (FOI) stained with antibodies against phospho-TOPK (p-TOPK) at Thr^{9} [30 FOIs per group, (C)], phosphohistone H3 at Ser^{10} [11 FOIs per group, (D)], Ki-67 [30 FOIs per group, (E)], and cleaved caspase-3 [15 FOIs per group, (F)]. Horizontal lines represent the means ± SD. Exact percentages of DAB-positive cells and P values are listed in table S2.

to be phosphorylated during mitosis and detected in the midbody at the end of mitosis (*5*, *17*, *18*). Autophosphorylation of TOPK ($P < 0.0001$; Fig. 5C and fig. S10A), as well as phosphorylation of histone H3 ($P < 0.0001$; Fig. 5D and fig. S10B), was significantly reduced in treated cells, indicating inhibition of the endogenous TOPK activity by this compound. Immunohistochemical staining with a cell proliferation marker (Ki-67) demonstrated suppression of LU-99 proliferation by the treatment ($P = 0.0001$; Fig. 5E and fig. S10C). In concordance with our previous findings after knockdown of TOPK, we observed an increase in cancer cell apoptosis (measured by cleaved caspase-3) in the tumors treated with liposomal OTS964 ($P < 0.0001$; Fig. 5F and fig. S10D). The phenotypic changes in cells, such as intercellular bridge and increased TUNEL (terminal deoxynucleotidyl transferase–mediated deoxyuridine triphosphate nick end labeling) staining, were more obvious in the tumor areas near blood vessels (fig. S11, A and B), supporting the EPR effect of the liposomal formulation of OTS964.

Oral administration of OTS964 in LU-99 xenograft model

Because OTS964 was expected to have higher bioavailability relative to its precursor drug, we next investigated the oral administration of OTS964, although the risk of hematopoietic toxicity was still a concern. The oral administration of free OTS964 at 50 or 100 mg/kg once every day for 2 weeks resulted in TGIs of 79 and 113% on day 15, respectively (Fig. 6A), without any body weight loss (Fig. 6B). Similar to the intravenous administration of liposomal OTS964, cell morphological changes, inhibition of TOPK activity, and increased cancer cell death were observed after oral administration of OTS964 for 1 week (figs. S12 and S13). In the 100 mg/kg dosing group, continuous tumor shrinkage was observed after the final administration of the drug, and all six of the mice achieved complete tumor regression (one on day 22, three on day 25, and two on day 29) (Fig. 6A). We did observe a significant decrease in the number of WBC 1 day after the final administration ($P < 0.01$; Fig. 6C), but the leukocytopenia spontaneously recovered 2 weeks later (Fig. 6D).

DISCUSSION

In the present study, we have demonstrated the therapeutic potential of TOPK inhibitors in mouse xenograft models of human lung cancer, as well as their suppressive effects on the growth of diverse types of human cancer cells. According to the Oncomine database (https://www.oncomine.org), the *TOPK* gene was shown to be frequently up-regulated in many types of cancer, including bladder, brain, breast, liver, and lung cancer, as well as sarcoma. Our Kaplan-Meier survival analyses of large data sets indicate that high expression of *TOPK* is correlated with poor prognosis for breast and lung cancer patients. In particular, because *TOPK* was very highly up-regulated (14-fold on average) in most of the 30 TNBCs examined (*9*), TOPK inhibitors should be considered as a possibility for TNBC patients who have limited therapeutic options.

Previous studies have suggested various molecular functions of TOPK in multiple signaling pathways, including MAPK (mitogen-activated protein kinase) pathway and NF-κB (nuclear factor κB) pathway (*19*–*21*). It was also suggested that TOPK might prevent cancer cell death by impairing the DNA damage–induced apoptosis pathway (*22*–*24*). However, TOPK was initially identified as a mitotic protein kinase (*25*), and accumulating reports have focused on critical roles of TOPK in cancer cell mitosis. The kinase activity of TOPK is elevated during mitosis, and TOPK promotes the phosphorylation of histone H3, PRC1 (protein regulator of cytokinesis 1), GPSM2 [G protein (heterotrimeric guanine nucleotide–binding protein) signaling modulator 2], and p97 proteins that are essential for completion of cancer cell cytokinesis (*8*, *26*, *27*). Therefore, it is likely that TOPK phosphorylates diverse protein substrates that are essential for cancer cell survival and proliferation, particularly in the mitotic phase of the cell cycle. Concordantly with previous reports (*5*, *8*), our results in human xenografts revealed that inhibition of TOPK activity with the liposomal OTS964 suppressed tumor growth through induction of cytokinesis defects and subsequent apoptosis. More importantly, our human xenograft studies demonstrated complete regression in five

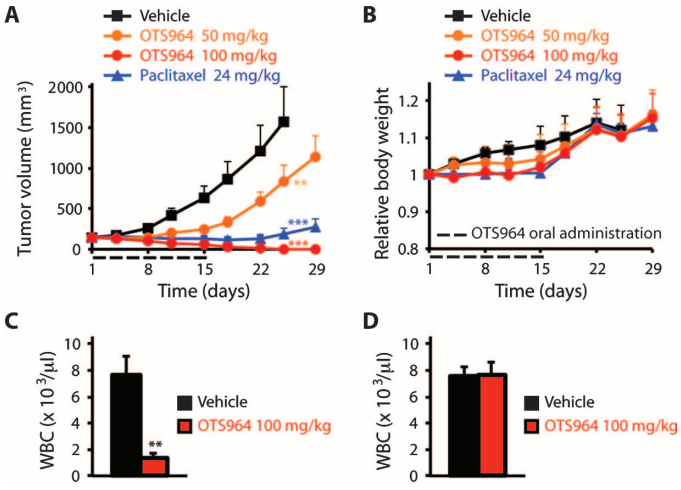

Fig. 6. Oral administration of OTS964 in lung cancer xenograft models. Nude mice bearing LU-99 were orally treated with vehicle control or free OTS964 or intravenously treated with paclitaxel. The free OTS964 was dosed at 50 and 100 mg/kg orally once every day for 2 weeks, whereas paclitaxel was given at 24 mg/kg on days 1, 4, 8, and 11. (**A**) Mean tumor volumes ± SD ($n = 6$ per treatment group) are shown. (**B**) Mean relative body weights ± SD ($n = 6$ per treatment group) in comparison with the mean body weight just before the administration (day 1) are shown. (**C** and **D**) Counting of WBCs was performed with a cell counting chamber on day 15 (C) and on day 29 (D), 2 weeks after the final administration of free OTS964 (100 mg/kg). $^{**}P < 0.01$ or $^{***}P < 0.001$ by *t* test. Original data and exact *P* values are provided in table S2.

of six tumors after only five shots of liposomal OTS964 with twice-a-week dosing. OTS964, which is an *N*, *N*-dimethylated derivative of OTS514, caused tumor shrinkage even after discontinuation of treatment and resulted in complete tumor regression, which was not observed with OTS514. One possible mechanism for the improved in vivo efficacy of OTS964 may be that the dimethylation modification reduced the efflux of this compound from cancer cells and therefore increased its intracellular concentration, as reported previously for other compounds (*28*, *29*). Furthermore, oral administration of free OTS964 once every day for 2 weeks led to complete regression of tumors in all six mice. These therapeutic effects can be distinguished from other mitotic kinase inhibitors under development, because most of them have shown TGI but rarely caused complete regression of tumors (*30*). Another group previously reported HI-TOPK-032 as a possible TOPK inhibitor and showed inhibition of tumor growth in mouse xenograft models of human colon cancer (*31*). However, HI-TOPK-032 revealed enzymatic IC_{50} as well as cellular IC_{50} for colon cancer cells at about 2 μM. Because most kinase inhibitors in clinical use have IC_{50} values at 50 nM or lower, this compound is far from clinical application. Our compounds showed very low cellular IC_{50}, ranging from 1.5 to 14.0 nM for OTS514 and from 7.6 to 73.0 nM for OTS964 in several types of cancer cell lines. Furthermore, treatment with liposomal OTS964 led to complete regression of LU-99 tumors, which has been rarely observed in other reported studies.

Although we first attempted to use TOPK inhibitors as free compounds to treat cancers, our xenograft models revealed that the free formulation of TOPK inhibitors caused severe hematopoietic abnormalities (decrease of RBCs and WBCs with a marked increase in platelets). We also observed in vitro that TOPK inhibitors enhanced the differentiation of HSCs to $CD41^+$ megakaryocytes, probably by suppressing differentiation into other lineages. Although we cannot exclude the possibility of off-target effects of our compounds, they are highly specific, as evident by the difference in IC_{50} for TOPK in comparison with other kinases that may play a role in hematopoiesis. Therefore, it is likely that TOPK plays a critical role in the differentiation of HSCs, and its inhibition enhances the differentiation of these cells into platelet progenitors, megakaryocytes. One signaling pathway that may be involved in this differentiation process is the STAT5 pathway. TOPK was previously reported to activate the NF-κB pathway, which is upstream of STAT5 (*21*, *32*), and we observed a reduction of STAT5 protein in HSCs after treatment with TOPK inhibitors. STAT5 is known to play an important role in the differentiation of HSCs into erythrocyte lineages, whereas its inactivation induces HSCs to differentiate into megakaryocytes (*33*). Therefore, our data suggest that TOPK inhibitors might directly or indirectly suppress the STAT5 function in HSCs and in turn skew the differentiation of HSCs toward megakaryocytes.

To reduce the hematopoietic toxicity and enhance drug concentration in the tumor tissue, we delivered the TOPK inhibitors in a liposomal formulation. Liposomal OTS964 showed slightly better TGI than paclitaxel (110 and 100% on day 22, respectively), but more importantly, it led to complete tumor regression with very minimum toxicity in mice. The liposomal formulation of compounds has proven to have advantages in cancer treatment, including suppression of adverse reactions in nontargeted tissues (*34*). Liposomal formulation promotes preferential accumulation of drugs from circulation in the tumor lesions, where capillary vessels are disrupted. For example, liposomal doxorubicin decreased cardiac and gastrointestinal toxicities as well as neutropenia (*35*, *36*). Similarly, in our xenograft models, we were able to completely prevent leukocytopenia by applying the liposomal formulation of TOPK inhibitors. In addition, our results demonstrate another advantage of the liposomal formulation of TOPK inhibitors: it enhanced drug effectiveness, likely by increasing the concentration of drug in tumor lesions, and thus achieved complete regression of tumors, which was not observed after treatment with the free drug.

We have demonstrated the therapeutic potential of TOPK-specific inhibitors in mouse xenograft models, but clinical trials in cancer patients will be essential to validate both the efficacy and the safety of these small molecular compounds. In addition, it remains unclear how TOPK-specific inhibitors enhance differentiation of HSCs to megakaryocytes and platelets. Nevertheless, this unexpected hematological effect might suggest additional clinical applications for these drugs in treating idiopathic thrombocytopenia or other hematological conditions, such as myelodysplastic syndromes, in which thrombocytopenia is one of the serious complications.

In summary, we have demonstrated the development of a liposomal formulation of a TOPK inhibitor that was shown to be effective in treating mouse xenograft models of cancer without any severe adverse events. Although oral administration of OTS964 caused some hematopoietic toxicity, this was a transient effect. Because we observed the spontaneous recovery from leukocytopenia and the anticancer effectiveness of the oral drug was similar to that of the liposomal formulation, oral administration of the drug may prove to be more practical. In conclusion, we believe that this compound is a promising therapeutic agent that may be applied to a wide range of human malignancies.

MATERIALS AND METHODS

Study design

This study was designed to investigate the therapeutic effects of newly developed TOPK-specific inhibitors delivered by intravenous injection of liposomal formulation or by oral administration of the free compounds. To examine the expression of TOPK protein in cancer cell lines, Western blot analyses were replicated. To assess growth inhibitory effects of TOPK-specific inhibitors in cancer cell lines, all assays were carried out in triplicate. We used two human lung cancer xenograft models in this study. When tumors reached sufficient size, animals were randomly assigned to the different treatment groups. All tumors' sizes were measured and graphed in figures without excluding any samples. For immunohistochemistry, all images obtained from treated or non-treated mice were blindly captured in the same setting on the microscope. DAB-positive cells were automatically scored by quantification software. Detailed information regarding sample number and replication in assays is provided in the following sections and figure legends. Detailed information on materials and methods, including synthesis of the compounds, kinase assay for compound screening, kinase specificity profile of TOPK inhibitors, time lapse microscopy, liposome preparation, immunohistochemistry of LU-99 xenograft, histopathological analysis, and image analysis, is given in Supplementary Materials.

Cell-based assay

Expression of TOPK and phosphorylation of histone H3 (Ser^{10}) were examined by Western blot, as described previously (*8*). Other antibodies used for Western blots are as follows: c-Src (1:1000, Cell Signaling Technology), Fyn (1:1000, Cell Signaling Technology), and Lyn (1:1000, Cell Signaling Technology). In vitro cell viability was measured by the colorimetric assay using Cell Counting Kit-8 (Dojindo Molecular Technologies Inc.). Cells (100 μl) were plated in 96-well plates at a density that generated continual linear growth (A549, 1×10^3 cells; LU-99, 2×10^3 cells; DU4475, 4×10^3 cells; MDA-MB-231, 3×10^3 cells; T47D, 3×10^3 cells; Daudi, 5×10^3 cells; UM-UC-3, 1×10^3 cells; HCT-116, 1×10^3 cells; MKN1, 2×10^3 cells; MKN45, 4×10^3 cells; HepG2, 4×10^3 cells; MIAPaca-2, 2×10^3 cells; 22Rv1, 6×10^3 cells; and HT29, 3×10^3 cells). The cells were allowed to adhere overnight before exposure to compounds for 72 hours at 37°C. Plates were read with a spectrophotometer at a wavelength of 450 nm. All assays were carried out in triplicate. After measuring IC_{50} values, we calculated the *z* scores to produce *P* values. After log transformation (base 10) of IC_{50} values (nM), the mean and SD were calculated for the log values of the IC_{50} for the 13 TOPK-positive cell lines. The mean and SD were 0.76 and 0.23 for OTS514 and 1.53 and 0.26 for OTS964. Then, the *z* scores from the HT29 IC_{50} values of OTS514 and OTS964 were 6.44 and 3.62, respectively.

In vivo xenograft study

A549 (1×10^7 cells) or LU-99 cells (5×10^6 or 1×10^7 cells) were injected subcutaneously in the left flank of female BALB/cSLC-nu/nu mice (Japan SLC Inc.). When A549 xenografts had reached an average volume of 200 mm^3 or when LU-99 xenografts had reached an average volume of 150 or 200 mm^3, animals were randomized into groups of six mice. The starting tumor volume of 150 mm^3 was used for LU-99 xenografts when tumors were monitored for a longer time period (>14 days), because LU-99 cells grew very rapidly, and thus the starting volume of 200 mm^3 prevented longer observation considering animal ethics (for example, 200 mm^3 of inoculated LU-99 tumor reached an average tumor volume of about 1100 mm^3, whereas A549 tumor reached about 490 mm^3 on day 15). For intravenous administration, compounds were formulated in 5% glucose and injected into the tail vein. For oral administration, compounds were prepared in a vehicle of 0.5% methylcellulose and given by oral gavage at the indicated dose and schedule. An administration volume of 10 ml/kg of body weight was used for both administration routes. Concentrations were indicated in the main text and figures. Tumor volumes were determined using a caliper. The results were converted to tumor volume (mm^3) by the formula length × $width^2$ × 1/2. The weight of the mice was determined as an indicator of tolerability on the same days. The animal experiments were conducted at KAC Co. Ltd. for A549 xenograft or at OncoTherapy Science Inc. for LU-99 xenograft, in accordance with the Institutional Guidelines for the Care and Use of Laboratory Animals of each site. TGI was calculated according to the formula $[1 - (T - T_0)/(C - C_0)] \times 100$, where T and T_0 are the mean tumor volumes at day 15 or 22 and day 1, respectively, for the experimental group, and C and C_0 are those for the vehicle control group. WBCs were counted with Sysmex XT-1800iV Analyzer (Sysmex Corporation) at KAC Co. Ltd. or with a cell counting chamber (ASONE) at OncoTherapy Science Inc. Blood was collected in a blood collection tube with EDTA (BD Biosciences) to prevent coagulation and to perform the blood cell count.

In vitro differentiation of human HSCs

$CD34^+$ HSCs (provided by W. Stock, The University of Chicago) were purified from growth factor–mobilized peripheral blood of healthy donors, and then cells were cultured in RPMI (Life Technologies) supplemented with 20% fetal bovine serum and 1× StemSpan CC100 (STEMCELL Technologies). Cells were treated with OTS514 (20 or 40 nM) or OTS964 (100 or 200 nM) for 48 hours. Collected cells were washed with phosphate-buffered saline (PBS) and resuspended in 100 μl of PBS followed by staining with CD41a antibody (eBioscience) for 20 min at room temperature. Finally, the cells were washed with PBS again and then analyzed for CD41a staining by flow cytometry on the BD FACSCalibur (BD Biosciences). Expression of STAT5 was examined by Western blot with an anti-STAT5 antibody (Cell Signaling Technology).

Kaplan-Meier survival analysis

We performed Kaplan-Meier survival analyses based on *TOPK* expression in breast and lung cancer patients using the Gene Expression Omnibus expression database and an online survival analysis tool, the Kaplan-Meier Plotter (*14*). Accession numbers for gene expression data sets were GSE-1456, -2034, -2990, -3493, -5327, -6532, -7390, -9195, -11121, -12093, -16391, and -12276 for breast cancer, and GSE-3141, -4573, -14814, -19188, -29013, -31210, and -37745 for lung cancer. Expression range of *TOPK* probe (219148_at) was 9 to 7205 in breast cancer data sets and 16 to 4732 in lung cancer data sets. The cutoff level (256 for breast cancer and 210 for lung cancer) of expression dividing TOPK-high and TOPK-low groups was determined by an algorithm of the Kaplan-Meier Plotter, and the overall survival rate was calculated for each data set of breast cancer (n =1115; follow-up for 20 years) and lung cancer (n = 1405; follow-up for 10 years).

Statistical analysis

Statistical analysis was performed with Prism 5 software (GraphPad Software Inc.). Sample sizes (at least six mice per treatment group) were chosen on the basis of previously published work. Detailed information

regarding sampling and normalization is described in the figure legends. All values in figures are presented as means ± SD. Original data and exact *P* values are provided in table S2. Statistical significance was calculated on the basis of Student's *t* test (two-tailed), *z* scores (difference in IC_{50}), or log-rank test (Kaplan-Meier survival analysis), and the level of significance was set at $P < 0.05$.

SUPPLEMENTARY MATERIALS

www.sciencetranslationalmedicine.org/cgi/content/full/6/259/259ra145/DC1
Materials and Methods
Fig. S1. Correlation between TOPK expression and clinical outcome.
Fig. S2. Cell-based antiproliferative assay for OTS514.
Fig. S3. LU-99 lung cancer xenograft model treated with intravenous administration of free OTS514.
Fig. S4. Cell-based antiproliferative assay for OTS964.
Fig. S5. Expression of Src family kinases in cancer cell lines.
Fig. S6. Inhibition of TOPK activity by OTS964 treatment.
Fig. S7. Enhancement of HSC differentiation to megakaryocytes by TOPK inhibitors.
Fig. S8. Histological examination of liver toxicity with liposomal OTS964.
Fig. S9. Cytokinetic defects in LU-99 cells after administration of liposomal OTS964.
Fig. S10. Effects of liposomal OTS964 on proliferation and death of cancer cells.
Fig. S11. Morphological changes and apoptosis of cancer cells after treatment with liposomal OTS964.
Fig. S12. LU-99 xenograft model treated by oral administration of free OTS964.
Fig. S13. Immunohistochemical staining of LU-99 tumor sections after oral administration of free OTS964.
Table S1. Kinase profile analysis of OTS514 and OTS964.
Table S2. Original data for composite figures from in vitro and in vivo experiments including *P* values (provided as a separate Excel file).
Video S1. Cytokinetic defect and apoptosis of T47D cells caused by OTS964 treatment.
Video S2. Normal proliferation of T47D cells.
References (*37*–*41*)

REFERENCES AND NOTES

1. R. Siegel, D. Naishadham, A. Jemal, Cancer statistics, 2013. *CA Cancer J. Clin.* **63**, 11–30 (2013).
2. C. DeSantis, J. Ma, L. Bryan, A. Jemal, Breast cancer statistics, 2013. *CA Cancer J. Clin.* **64**, 52–62 (2014).
3. D. M. Keefe, E. H. Bateman, Tumor control versus adverse events with targeted anticancer therapies. *Nat. Rev. Clin. Oncol.* **9**, 98–109 (2011).
4. A. Mohamed, K. Krajewski, B. Cakar, C. X. Ma, Targeted therapy for breast cancer. *Am. J. Pathol.* **183**, 1096–1112 (2013).
5. J. H. Park, M. L. Lin, T. Nishidate, Y. Nakamura, T. Katagiri, PDZ-binding kinase/T-LAK cell-originated protein kinase, a putative cancer/testis antigen with an oncogenic activity in breast cancer. *Cancer Res.* **66**, 9186–9195 (2006).
6. M. C. Shih, J. Y. Chen, Y. C. Wu, Y. H. Jan, B. M. Yang, P. J. Lu, H. C. Cheng, M. S. Huang, C. J. Yang, M. Hsiao, J. M. Lai, TOPK/PBK promotes cell migration via modulation of the PI3K/PTEN/AKT pathway and is associated with poor prognosis in lung cancer. *Oncogene* **31**, 2389–2400 (2012).
7. P. C. O'Leary, S. A. Penny, R. T. Dolan, C. M. Kelly, S. F. Madden, E. Rexhepaj, D. J. Brennan, A. H. McCann, F. Pontén, M. Uhlén, R. Zagozdzon, M. J. Duffy, M. R. Kell, K. Jirström, W. M. Gallagher, Systematic antibody generation and validation via tissue microarray technology leading to identification of a novel protein prognostic panel in breast cancer. *BMC Cancer* **13**, 175 (2013).
8. J. H. Park, T. Nishidate, Y. Nakamura, T. Katagiri, Critical roles of T-LAK cell-originated protein kinase in cytokinesis. *Cancer Sci.* **101**, 403–411 (2010).
9. M. Komatsu, T. Yoshimaru, T. Matsuo, K. Kiyotani, Y. Miyoshi, T. Tanahashi, K. Rokutan, R. Yamaguchi, A. Saito, S. Imoto, S. Miyano, Y. Nakamura, M. Sasa, M. Shimada, T. Katagiri, Molecular features of triple negative breast cancer cells by genome-wide gene expression profiling analysis. *Int. J. Oncol.* **42**, 478–506 (2013).
10. I. Shats, M. L. Gatza, J. T. Chang, S. Mori, J. Wang, J. Rich, J. R. Nevins, Using a stem cell–based signature to guide therapeutic selection in cancer. *Cancer Res.* **71**, 1772–1780 (2011).
11. Y. Nakamura, Y. Matsuo, S. Hisada, F. Ahmed, R. Huntley, Z. Sajjadi-Hashemi, D. M. Jenkins, R. B. Kargbo, W. Cui, P. F. Gauuan, J. R. Walker, H. Decornez, M. Gurram, Tricyclic compounds and PBK inhibitors containing the same. Patent WO/2011/123419 (2011).
12. Y. Matsumura, Cancer stromal targeting (CAST) therapy. *Adv. Drug Deliv. Rev.* **64**, 710–719 (2012).
13. H. I. Chang, M. K. Yeh, Clinical development of liposome-based drugs: Formulation, characterization, and therapeutic efficacy. *Int. J. Nanomedicine* **7**, 49–60 (2012).
14. B. Győrffy, A. Lanczky, A. C. Eklund, C. Denkert, J. Budczies, Q. Li, Z. Szallasi, An online survival analysis tool to rapidly assess the effect of 22,277 genes on breast cancer prognosis using microarray data of 1,809 patients. *Breast Cancer Res. Treat.* **123**, 725–731 (2010).
15. B. Győrffy, P. Surowiak, J. Budczies, A. Lánczky, Online survival analysis software to assess the prognostic value of biomarkers using transcriptomic data in non-small-cell lung cancer. *PLOS One* **8**, e82241 (2013).
16. N. Elia, C. Ott, J. Lippincott-Schwartz, Incisive imaging and computation for cellular mysteries: Lessons from abscission. *Cell* **155**, 1220–1231 (2013).
17. C. Prigent, S. Dimitrov, Phosphorylation of serine 10 in histone H3, what for? *J. Cell Sci.* **116**, 3677–3685 (2003).
18. D. W. Li, Q. Yang, J. T. Chen, H. Zhou, R. M. Liu, X. T. Huang, Dynamic distribution of Ser-10 phosphorylated histone H3 in cytoplasm of MCF-7 and CHO cells during mitosis. *Cell Res.* **15**, 120–126 (2005).
19. Y. Abe, S. Matsumoto, K. Kito, N. Ueda, Cloning and expression of a novel MAPKK-like protein kinase, lymphokine-activated killer T-cell-originated protein kinase, specifically expressed in the testis and activated lymphoid cells. *J. Biol. Chem.* **275**, 21525–21531 (2000).
20. F. Zhu, T. A. Zykova, B. S. Kang, Z. Wang, M. C. Ebeling, Y. Abe, W. Y. Ma, A. M. Bode, Z. Dong, Bidirectional signals transduced by TOPK-ERK interaction increase tumorigenesis of HCT116 colorectal cancer cells. *Gastroenterology* **133**, 219–231 (2007).
21. J. H. Park, D. S. Yoon, H. J. Choi, D. H. Hahm, S. M. Oh, Phosphorylation of IκBα at serine 32 by T-lymphokine-activated killer cell-originated protein kinase is essential for chemoresistance against doxorubicin in cervical cancer cells. *J. Biol. Chem.* **288**, 3585–3593 (2013).
22. V. Ayllón, R. O'connor, PBK/TOPK promotes tumour cell proliferation through p38 MAPK activity and regulation of the DNA damage response. *Oncogene* **26**, 3451–3461 (2007).
23. F. Hu, R. B. Gartenhaus, D. Eichberg, Z. Liu, H. B. Fang, A. P. Rapoport, PBK/TOPK interacts with the DBD domain of tumor suppressor p53 and modulates expression of transcriptional targets including p21. *Oncogene* **29**, 5464–5474 (2010).
24. S. Li, F. Zhu, T. Zykova, M. O. Kim, Y. Y. Cho, A. M. Bode, C. Peng, W. Ma, A. Carper, A. Langfald, Z. Dong, T-LAK cell-originated protein kinase (TOPK) phosphorylation of MKP1 protein prevents solar ultraviolet light-induced inflammation through inhibition of the p38 protein signaling pathway. *J. Biol. Chem.* **286**, 29601–29609 (2011).
25. S. Gaudet, D. Branton, R. A. Lue, Characterization of PDZ-binding kinase, a mitotic kinase. *Proc. Natl. Acad. Sci. U.S.A.* **97**, 5167–5172 (2000).
26. Y. Abe, T. Takeuchi, L. Kagawa-Miki, N. Ueda, K. Shigemoto, M. Yasukawa, K. Kito, A mitotic kinase TOPK enhances Cdk1/cyclin B1-dependent phosphorylation of PRC1 and promotes cytokinesis. *J. Mol. Biol.* **370**, 231–245 (2007).
27. C. Fukukawa, K. Ueda, T. Nishidate, T. Katagiri, Y. Nakamura, Critical roles of LGN/GPSM2 phosphorylation by PBK/TOPK in cell division of breast cancer cells. *Genes Chromosomes Cancer* **49**, 861–872 (2010).
28. A. Schaefer, J. Westendorf, K. Lingelbach, C. A. Schmidt, D. L. Mihalache, A. Reymann, H. Marquardt, Decreased resistance to *N*,*N*-dimethylated anthracyclines in multidrug-resistant Friend erythroleukemia cells. *Cancer Chemother. Pharmacol.* **31**, 301–307 (1993).
29. L. Gate, P. Couvreur, G. Nguyen-Ba, H. Tapiero, *N*-methylation of anthracyclines modulates their cytotoxicity and pharmacokinetic in wild type and multidrug resistant cells. *Biomed. Pharmacother.* **57**, 301–308 (2003).
30. E. Komlodi-Pasztor, D. L. Sackett, A. T. Fojo, Inhibitors targeting mitosis: Tales of how great drugs against a promising target were brought down by a flawed rationale. *Clin. Cancer Res.* **18**, 51–63 (2012).
31. D. J. Kim, Y. Li, K. Reddy, M. H. Lee, M. O. Kim, Y. Y. Cho, S. Y. Lee, J. E. Kim, A. M. Bode, Z. Dong, Novel TOPK inhibitor HI-TOPK-032 effectively suppresses colon cancer growth. *Cancer Res.* **72**, 3060–3068 (2012).
32. M. Hinz, P. Lemke, I. Anagnostopoulos, C. Hacker, D. Krappmann, S. Mathas, B. Dörken, M. Zenke, H. Stein, C. Scheidereit, Nuclear factor κB–dependent gene expression profiling of Hodgkin's disease tumor cells, pathogenetic significance, and link to constitutive signal transducer and activator of transcription 5a activity. *J. Exp. Med.* **196**, 605–617 (2002).
33. S. G. Olthof, S. Fatrai, A. L. Drayer, M. R. Tyl, E. Vellenga, J. J. Schuringa, Downregulation of signal transducer and activator of transcription 5 (STAT5) in $CD34^+$ cells promotes megakaryocytic development, whereas activation of STAT5 drives erythropoiesis. *Stem Cells* **26**, 1732–1742 (2008).
34. J. Lao, J. Madani, T. Puértolas, M. Alvarez, A. Hernández, R. Pazo-Cid, A. Artal, A. Antón Torres, Liposomal doxorubicin in the treatment of breast cancer patients: A review. *J. Drug Deliv.* **2013**, 456409 (2013).
35. M. R. Ranson, J. Carmichael, K. O'Byrne, S. Stewart, D. Smith, A. Howell, Treatment of advanced breast cancer with sterically stabilized liposomal doxorubicin: Results of a multicenter phase II trial. *J. Clin. Oncol.* **15**, 3185–3191 (1997).

36. S. M. Rafiyath, M. Rasul, B. Lee, G. Wei, G. Lamba, D. Liu, Comparison of safety and toxicity of liposomal doxorubicin vs. conventional anthracyclines: A meta-analysis. *Exp. Hematol. Oncol.* **1**, 10 (2012).
37. J. R. Sportsman, E. A. Gaudet, A. Boge, Immobilized metal ion affinity-based fluorescence polarization (IMAP): Advances in kinase screening. *Assay Drug Dev. Technol.* **2**, 205–214 (2004).
38. T. Anastassiadis, S. W. Deacon, K. Devarajan, H. Ma, J. R. Peterson, Comprehensive assay of kinase catalytic activity reveals features of kinase inhibitor selectivity. *Nat. Biotechnol.* **29**, 1039–1045 (2011).
39. C. A. Schneider, W. S. Rasband, K. W. Eliceiri, NIH Image to ImageJ: 25 years of image analysis. *Nat. Methods* **9**, 671–675 (2012).
40. F. Szoka, F. Olson, T. Heath, W. Vail, E. Mayhew, D. Papahadjopoulos, Preparation of unilamellar liposomes of intermediate size (0.1-0.2 mumol) by a combination of reverse phase evaporation and extrusion through polycarbonate membranes. *Biochim. Biophys. Acta* **601**, 559–571 (1980).
41. V. J. Tuominen, S. Ruotoistenmäki, A. Viitanen, M. Jumppanen, J. Isola, ImmunoRatio: A publicly available web application for quantitative image analysis of estrogen receptor (ER), progesterone receptor (PR), and Ki-67. *Breast Cancer Res.* **12**, R56 (2010).

Acknowledgments: We thank K. Adachi, K. Toyota, and M. Mutonga for technical support, T. Katagiri for helpful discussion, and W. Stock for providing human HSCs. **Funding:** This work was supported in part by the Innovation Promotion Program of the New Energy and Industrial Technology Development Organization of Japan and OncoTherapy Science Inc. **Author contributions:** Y.N. planned and supervised the entire project. Y.M. contributed to the planning of the discovery research and the compound design. J.-H.P. and Y.N. performed functional study in tumor and analyzed data. T.M., S.Y., and S.H. contributed to most in vitro and in vivo experiments using TOPK inhibitors. H.A. performed experiments using HSCs. Y.M., J.-H.P., and Y.N. wrote the manuscript. **Competing interests:** Y.M., T.M., S.Y., and S.H. are employees of OncoTherapy Science Inc. J.-H.P. is a scientific adviser of OncoTherapy Science Inc. Y.N. is a stockholder and an adviser of OncoTherapy Science Inc. A patent application (WO/2011/123419) has been filed for compounds OTS514 and OTS964. **Data and materials availability:** OTS514 and OTS964 can be obtained through material transfer agreement from OncoTherapy Science Inc.

Submitted 6 August 2014
Accepted 23 September 2014
Published 22 October 2014
10.1126/scitranslmed.3010277

Citation: Y. Matsuo, J.-H. Park, T. Miyamoto, S. Yamamoto, S. Hisada, H. Alachkar, Y. Nakamura, TOPK inhibitor induces complete tumor regression in xenograft models of human cancer through inhibition of cytokinesis. *Sci. Transl. Med.* **6**, 259ra145 (2014).